

## Vanishing Confinement Regime in Terahertz HgTe Nanocrystals Studied under Extreme Conditions of Temperature and Pressure

Stefano Pierini<sup>1,2</sup>, Francesco Capitani<sup>3</sup>, Michael Scimeca<sup>4</sup>, Sergei Kozlov<sup>5</sup>, Debora Pierucci<sup>2</sup>, Rodolphe Alchaar<sup>1</sup>, Claire Abadie<sup>1</sup>, Adrien Khalili<sup>1</sup>, Mariarosa Cavallo<sup>1</sup>, Tung Huu Dang<sup>1</sup>, Huichen Zhang<sup>1</sup>, Erwan Bossavit<sup>1</sup>, Charlie Gréboval<sup>1</sup>, José Avila<sup>3</sup>, Benoit Baptiste<sup>6</sup>, Stefan Klotz<sup>6</sup>, Ayaskanta Sahu<sup>4</sup>, Cheryl Feuillet-Palma<sup>5</sup>, Xiang Zhen Xu<sup>5</sup>, Abdelkarim Ouerghi<sup>2</sup>, Sandrine Ithurria<sup>5</sup>, James K. Utterback<sup>1</sup>, Sebastien Sauvage<sup>2</sup>, Emmanuel Lhuillier<sup>1\*</sup>

<sup>1</sup> Sorbonne Université, CNRS, Institut des NanoSciences de Paris, INSP, F-75005 Paris, France.

<sup>2</sup> Université Paris-Saclay, CNRS, Centre de Nanosciences et de Nanotechnologies, CNRS, 10 Boulevard Thomas Gobert, 91120 Palaiseau, France

<sup>3</sup> Synchrotron-SOLEIL, Saint-Aubin, BP48, F91192 Gif sur Yvette Cedex, France.

<sup>4</sup> Department of Chemical and Biomolecular Engineering, New York University, Brooklyn, NY 11201, USA

<sup>5</sup> Laboratoire de Physique et d'Etude des Matériaux, ESPCI-Paris, PSL Research University, Sorbonne Université Univ Paris 06, CNRS UMR 8213, 10 rue Vauquelin 75005 Paris, France.

<sup>6</sup> Sorbonne Université, CNRS, Institut de Minéralogie, de Physique des Matériaux et de Cosmochimie, IMPMC, F-75005 Paris, France.

\*To whom correspondence should be sent: [el@insp.upmc.fr](mailto:el@insp.upmc.fr)

### Table of content

1. <b>Material characterization</b> .....	2
2. <b>Transport at high temperature</b> .....	5
3. <b>X-ray diffraction under pressure</b> .....	6
4. <b>Infrared transmission under pressure</b> .....	8
5. <b>kp modelling of the zinc blende phase electronic structure</b> .....	11
6. <b>REFERENCES</b> .....	12

## 1. Material characterization

- **Particle size distribution**

From electron microscopy we have determined the particle size. The mean size is coherent with the one determined by X-ray diffraction, see **Figure S 5**.

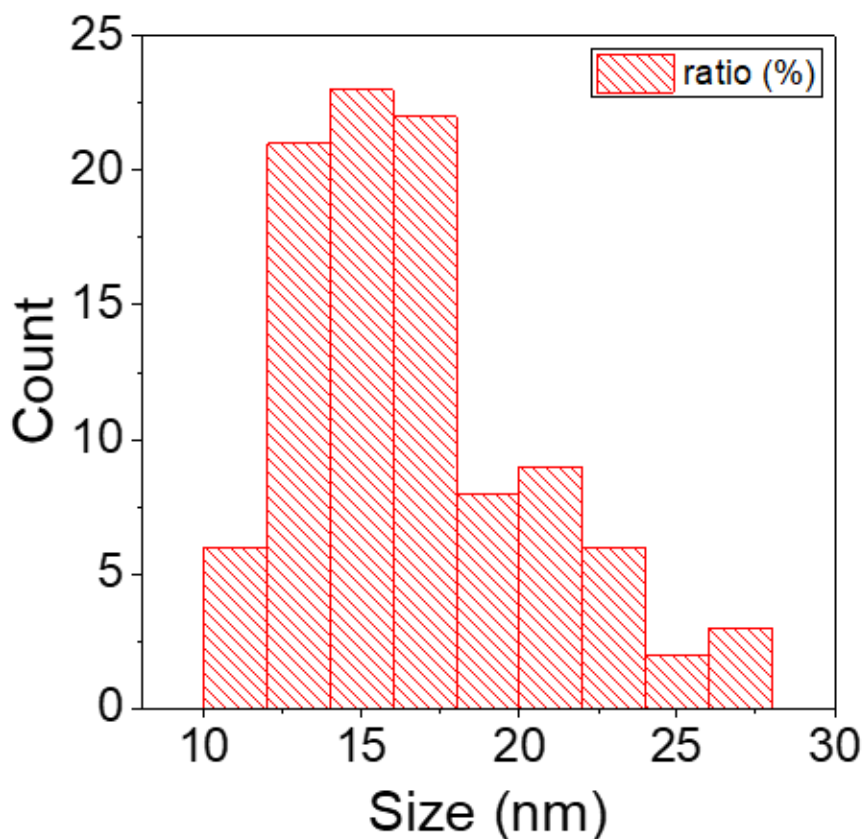


**Figure S 1 Particle size distribution** obtained from transmission electron microscopy

- **Particle surface chemistry**

**Figure S 2** shows the infrared spectrum of the HgTe THz NC as well as the absorbance from solutions of dodecanethiol and oleylamine. The latter are used as ligands and coordinating solvents during the synthesis. The three sharp lines observed in the HgTe NC absorbance spectrum can indeed be attributed to the capping ligands. Also note that in the mid IR, additional features due to C-H and N-H are observed.

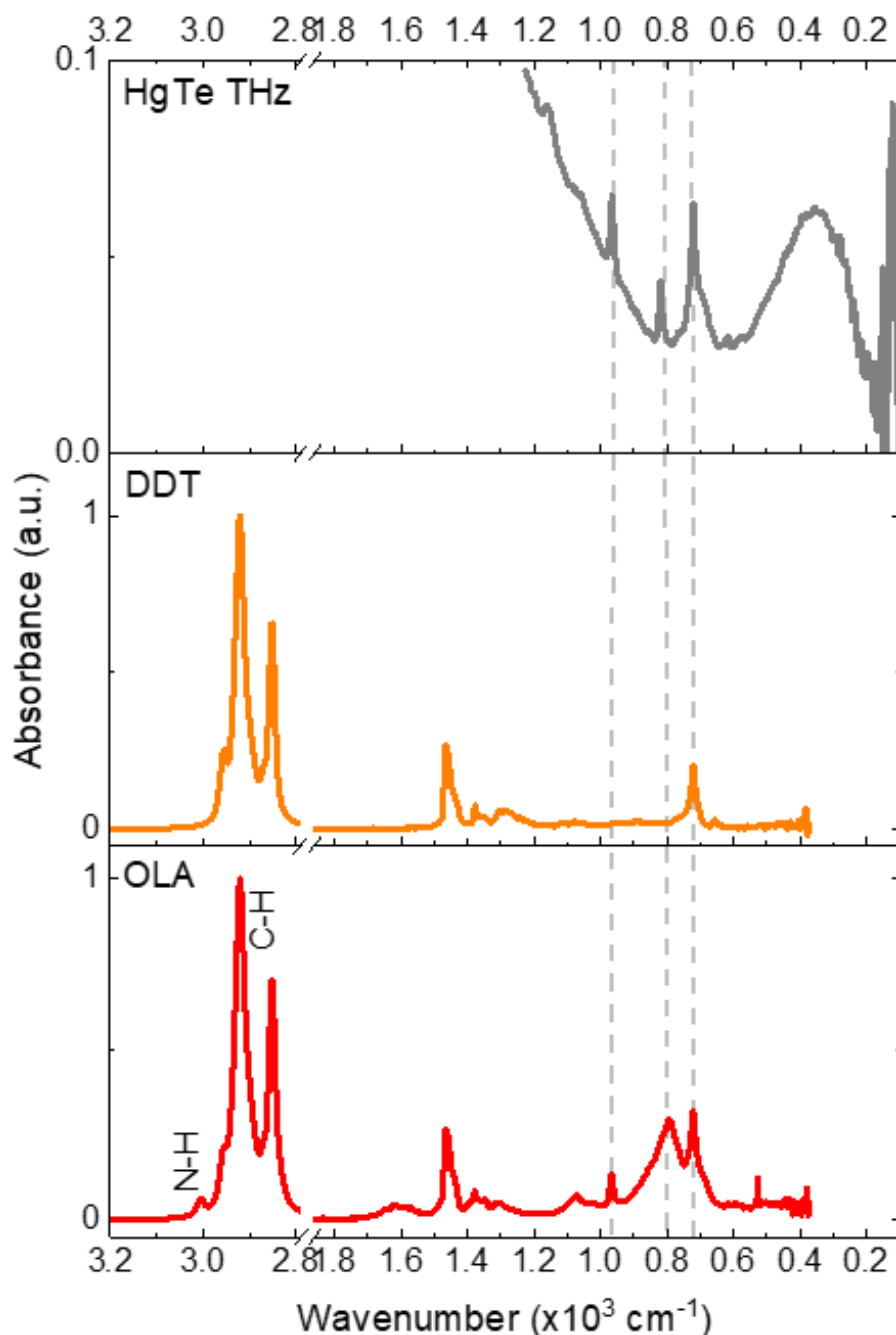


**Figure S 2** Infrared spectrum of HgTe THz NCs and from dodecanethiol (DDT) and oleylamine (OLA) used as ligands during the synthesis.

To further characterize the material surface chemistry, we have used X-ray photoemission spectroscopy. The survey spectrum (**Figure S 3a**) shows features from Hg, Te, C, O, S and also gold from the substrate. The Hg 4f state (**Figure S 3b**) displays two features that are respectively attributed to Hg bound to Te and Hg bound to S coming from the ligands<sup>1</sup>. The Te states (3d and 4d in **Figure S 3c** and d) present a single contribution. We can thus exclude any oxidation of the material which is consistent with the weak O 1s peak observed that can be attributed to air

preparation of the sample. The feature from S and C (**Figure S 3e** and **f**) relates to the dodocanethiol used as ligands.

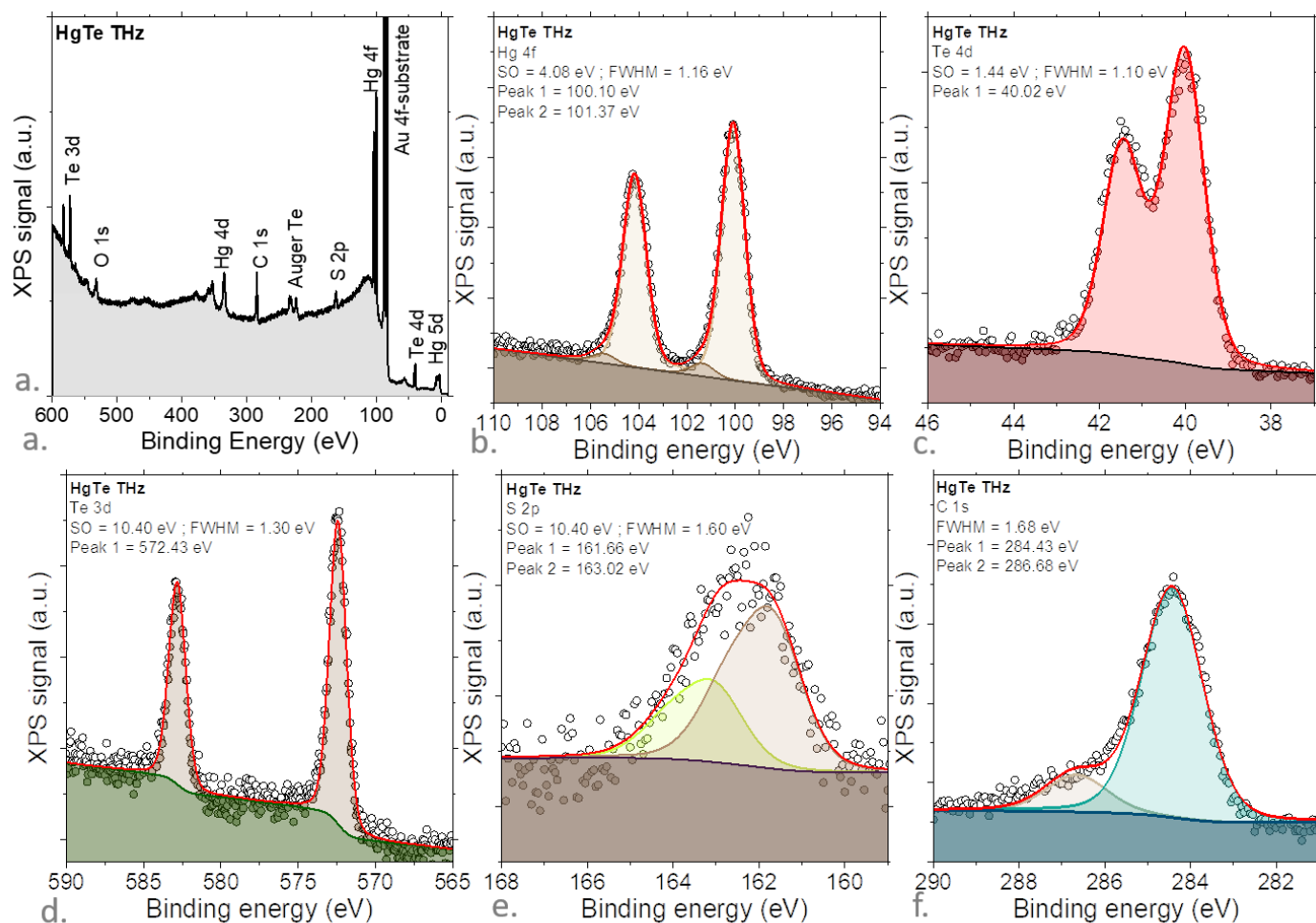


**Figure S 3 Photoemission spectrum.** a. overview spectrum for a HgTe NC film acquired for a 700 eV photon energy. core level (b-Hg4f, c, Te 4d, d-Te 3d, e-S2p, f-C1s).

## 2. Transport at high temperature

While Figure 2 in the main text provides the data relative to transport at low temperature, I-V curves in the high temperature range (here 16 K to room temperature) are given in **Figure S 4**. All curves are linear.

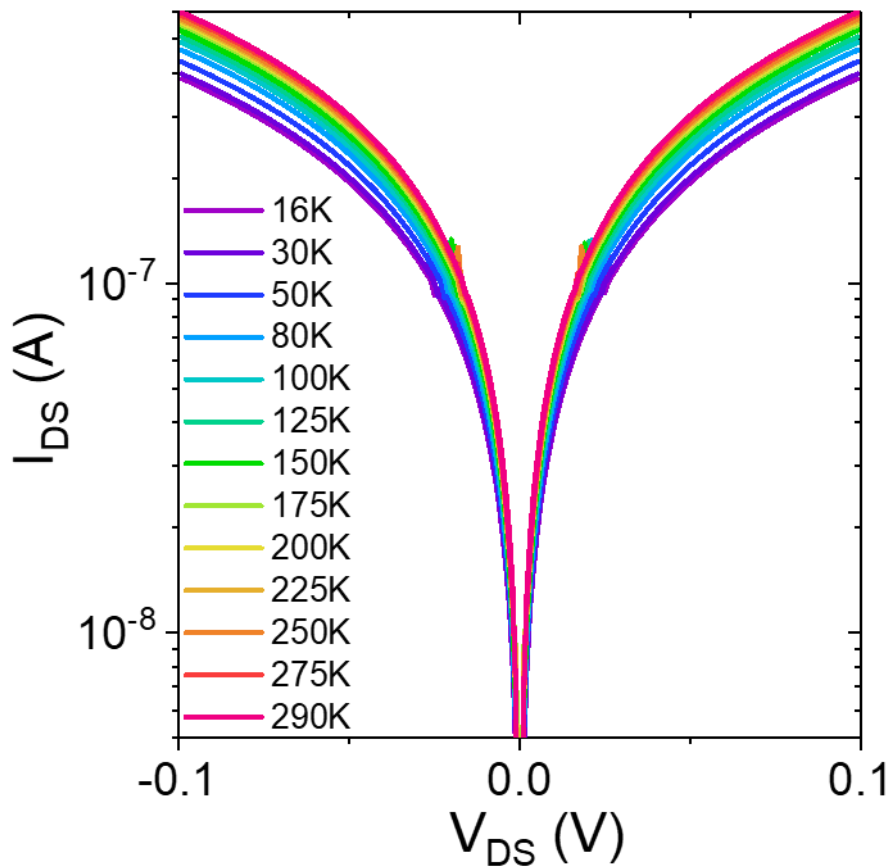


**Figure S 4** IV curves at different temperatures from 16 K to room temperature.

### 3. X-ray diffraction under pressure

**Figure S 5** shows diffraction patterns under various applied pressures, while the data of the difference phases have been split.

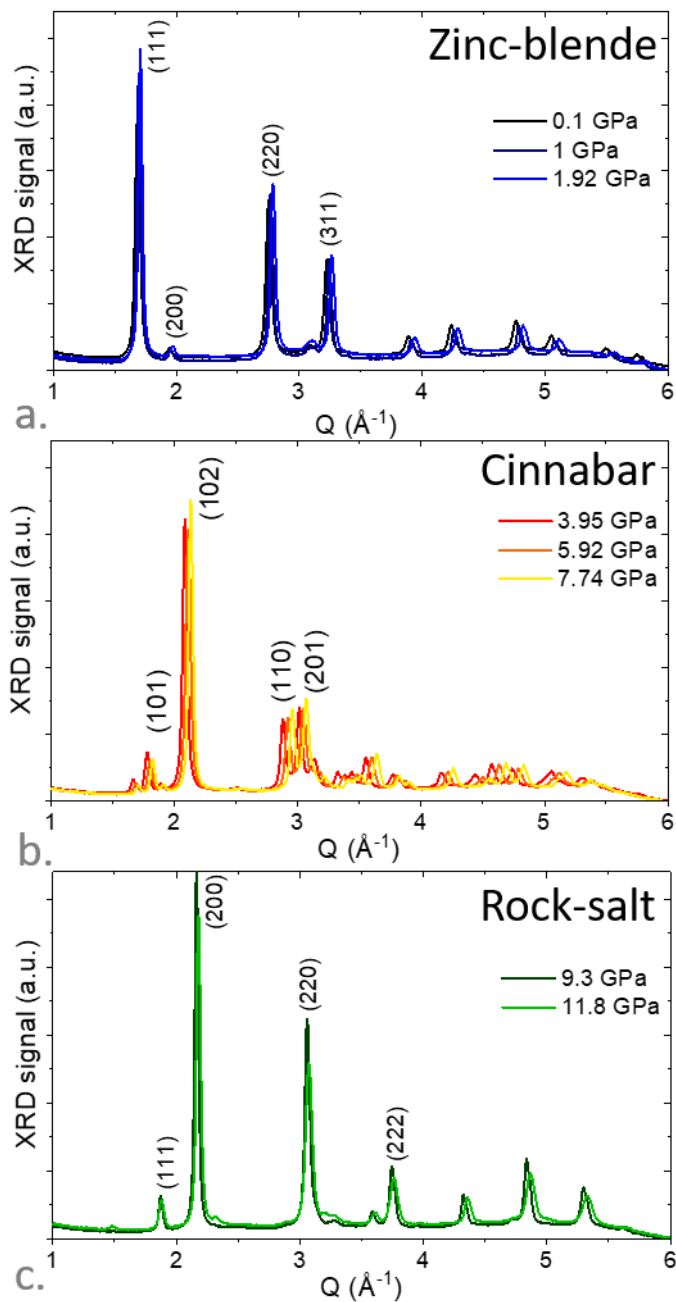


**Figure S 5** Diffraction patterns under various applied pressures for HgTe THz NCs, in the zinc blende phase (a.), in the cinnabar phase (b.) and in the rock-salt phase (c.).

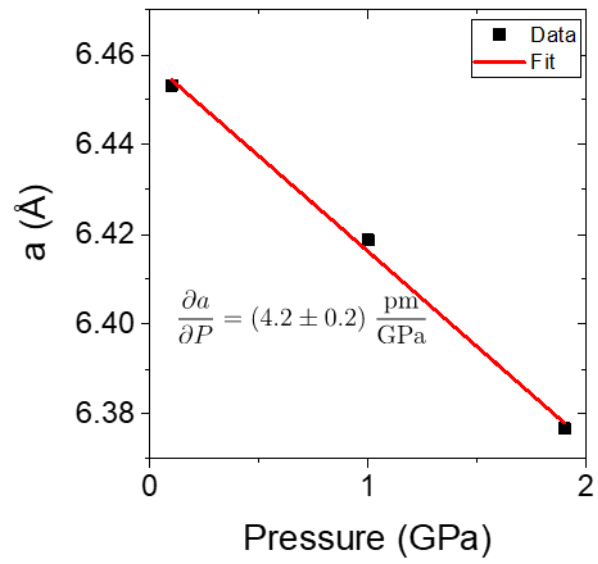


**Figure S 6 Zinc blende lattice parameter as a function of the applied pressure.**

## 4. Infrared transmission under pressure

**Figure S 7** shows the broad band setup used to apply pressure and measure the absorption spectrum in the infrared range.

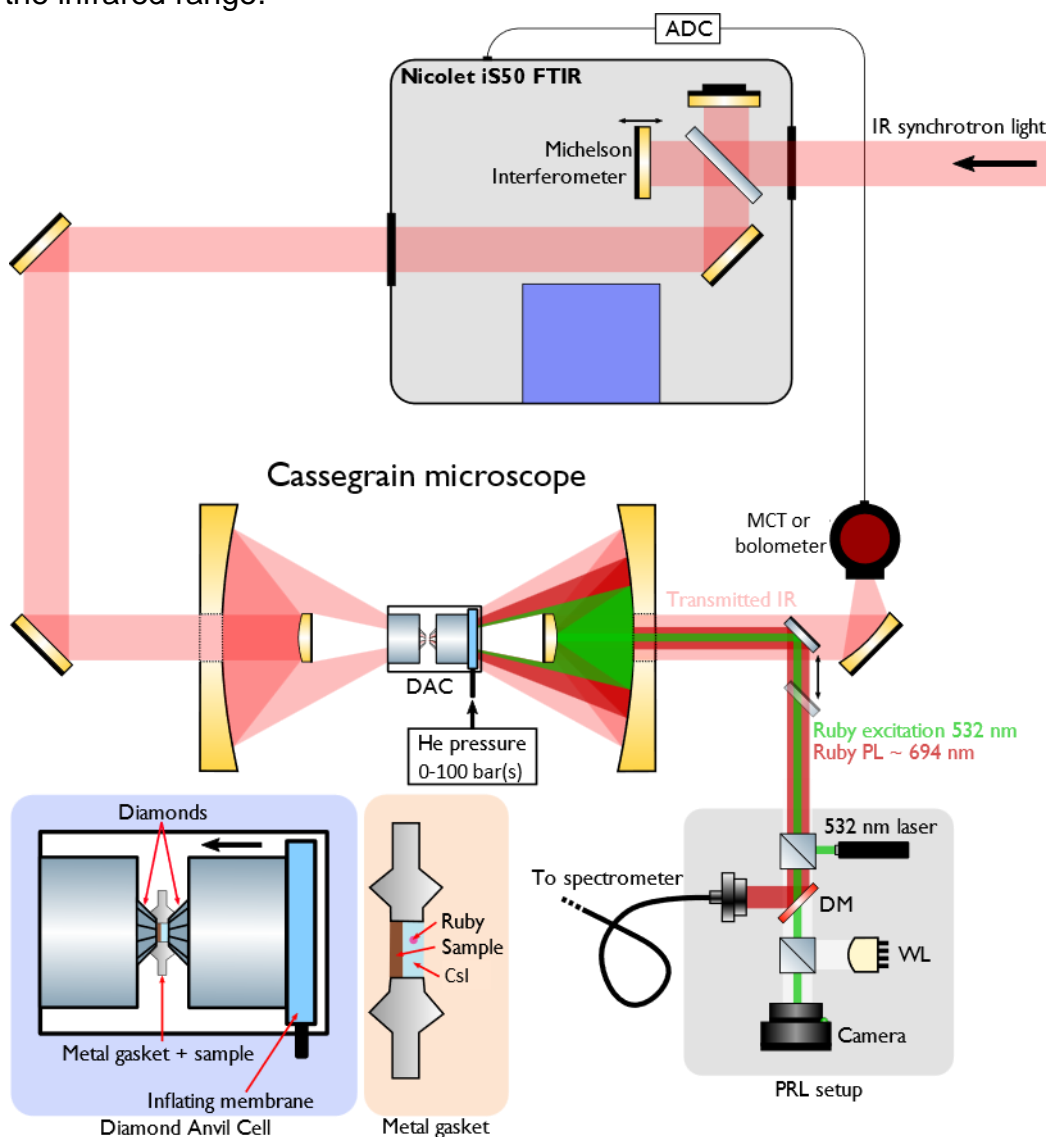


**Figure S 7 Scheme of the optical setup used to obtain infrared spectra of the HgTe nanocrystals under pressure.** Synchrotron light is used as a broad band infrared source. The pressure within the diamond cell is measured through the shift of the ruby luminescence. DAC: Diamond Anvil Cell. PRL: Pressure by Ruby Luminescence spectrometer. DM: Dichroic Mirror. The figure is adapted with permission from ref<sup>2</sup> Copyright {2019} American Chemical Society.

## Spectrum processing for Infrared spectroscopy under pressure

The procedure used to process the raw infrared spectrum is described in Figure S 8.

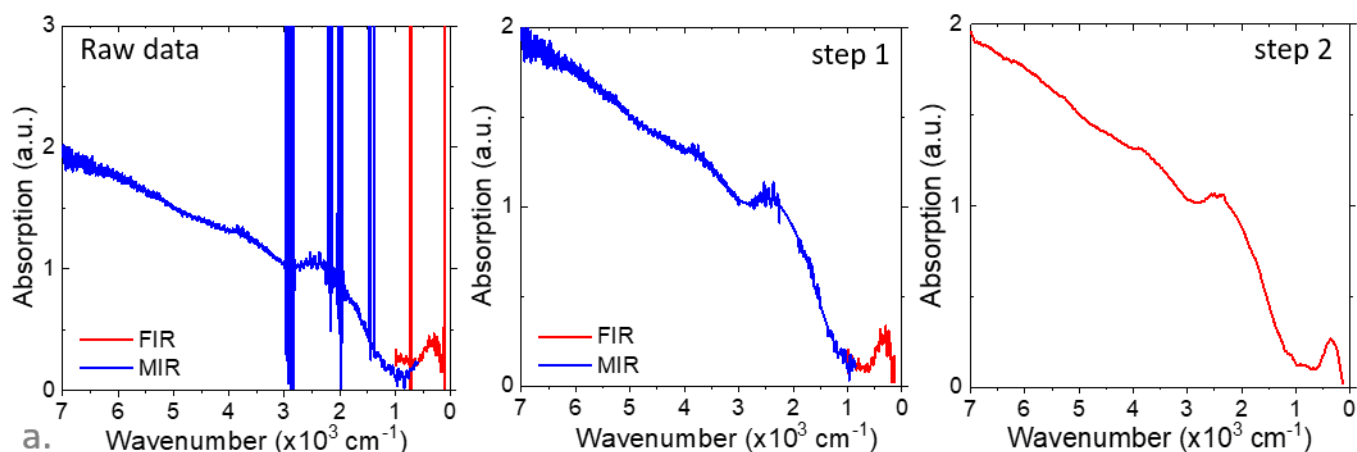


**Figure S 8 Spectrum processing.** a. raw spectra as collected on MCT for mid infrared part and on bolometer for far infrared part. b. the same data are shown as they appear after the first step of processing (i.e. removing of the noise due to absence of signal in certain regions). c. the same data are shown as they appear after the smoothing with a Savitzky-Golay filter.

The raw spectral data appears in **Figure S 8a**: we observe several narrow ranges where the signal is noisy. This is due to the presence of the absorption of polyethylene (cryostat windows), diamonds or PE (bolometer window). To have more readable data, we decided to remove these parts and replace them with a second order polynomial fit performed on the adjacent region. In addition, we removed the data between 7000 and 8000  $\text{cm}^{-1}$  where we did not have enough signal. The result of this operation (step 1, in **Figure S 8b**) is shown in the central figure, where the data is more readable. As all the information we look for has large peaks, the data is then merged and smoothed using a Savitzky-Golay filter<sup>3</sup> (step 2 in **Figure S 8c**).

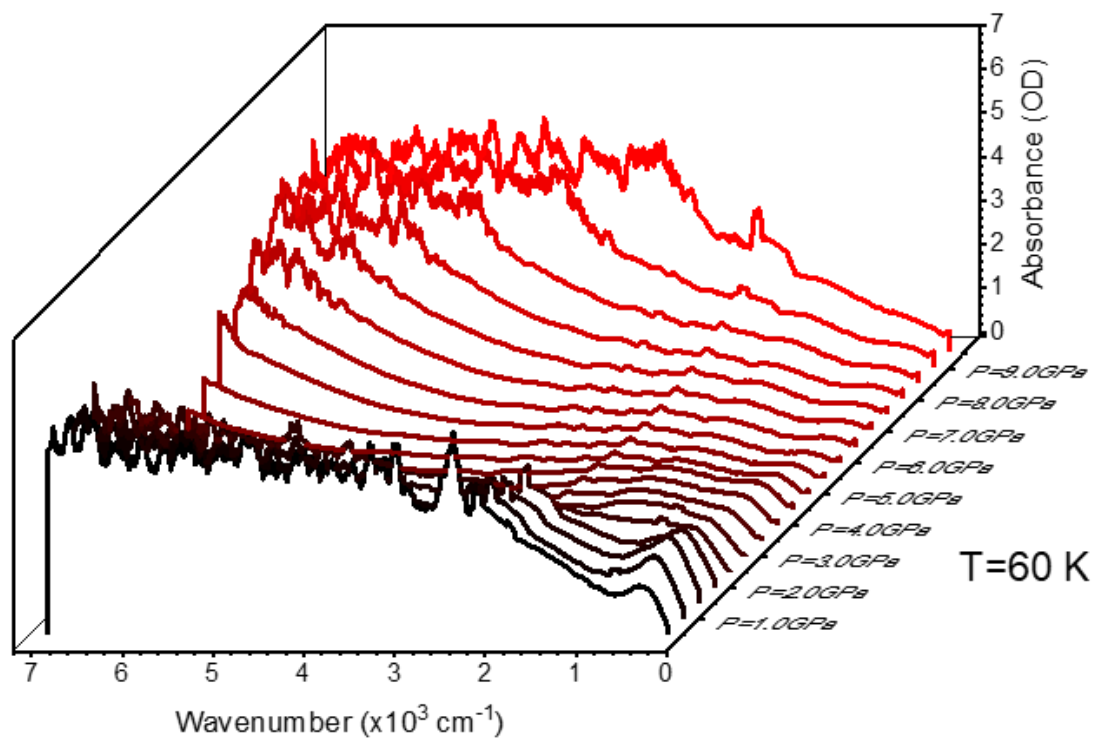


**Figure S 9. Infrared spectra for THz HgTe NCs under various pressures, made at 60 K.**

## 5. kp modelling of the zinc blende phase electronic structure

**Figure S10a** presents the absorbance spectra in the 0-3.5 GPa pressure range from Figure 5. In the corresponding zinc-blende phase, we clearly observe a blue-shift of the absorption with pressure. Considering an absorbance of 1.5, we extract for the zinc-blende phase an experimental  $30 \text{ meV.GPa}^{-1}$  blue shift as shown by the squares and the dotted line in **Figure S10b**. We now compare this pressure coefficient to a modeling of the absorption. In a previous article,<sup>4</sup> we investigated the pressure dependence of interband absorption of highly confined nanocrystals and nanoplatelets, exhibiting typical energies around 0.26-1.8 eV range. We use the 14-band modeling of the electronic structure of reference<sup>4</sup> and *exactly* the same parameter set. From the model, we extract a pressure coefficient of  $32 \text{ meV.GPa}^{-1}$  at 60 K as shown in **Figure S10b** by the full lines at different temperatures, significantly smaller than the one of smaller nanocrystals ( $60 \text{ meV.GPa}^{-1}$ ) but close to the one we observe in Figure 5.

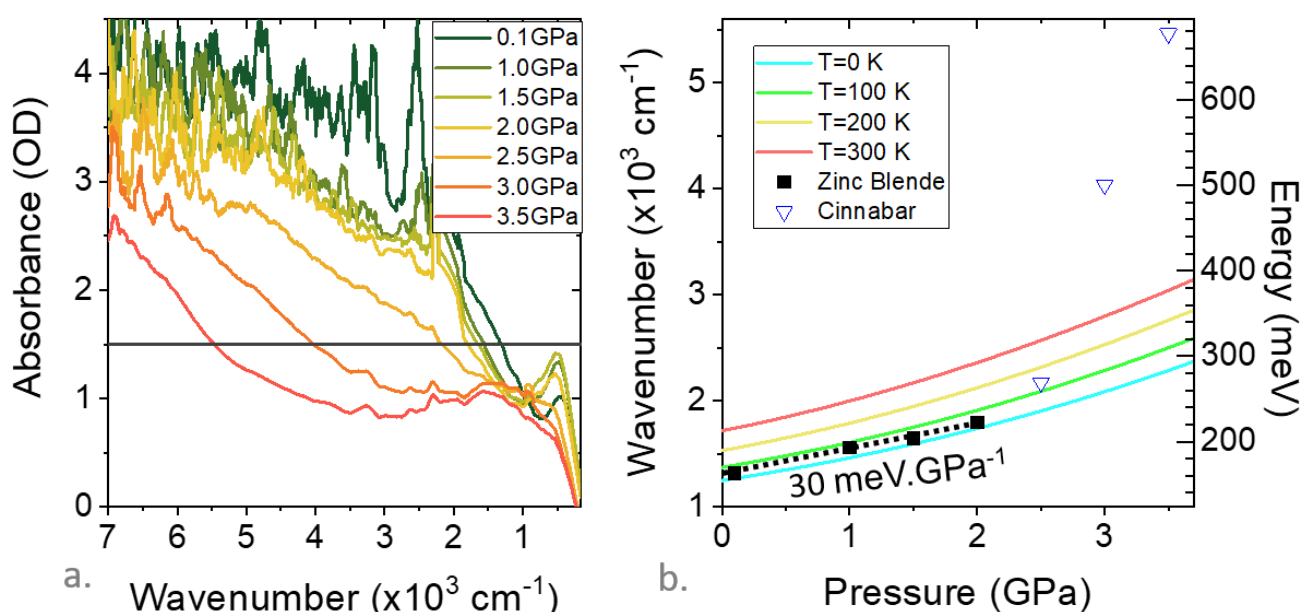


**Figure S10 kp Modeling of the zinc blende phase.** *a.* Absorption spectra for the zinc-blende phase at pressures from 0 to 3.7 GPa. *b.* Interband absorption wavenumber at 1.5 absorbance (squares and triangles) and simulation from the 14-band *k.p* modeling of the absorption (full colored lines). A pressure shift of  $30 \text{ meV.GPa}^{-1}$  is measured for the zinc-blende phase (dotted line), close the  $32 \text{ meV.GPa}^{-1}$  simulated one.

## 6. REFERENCES

- (1) Gréboval, C.; Chu, A.; Goubet, N.; Livache, C.; Ithurria, S.; Lhuillier, E. Mercury Chalcogenide Quantum Dots: Material Perspective for Device Integration. *Chem. Rev.* **2021**, *121*, 3627–3700.
- (2) Livache, C.; Goubet, N.; Gréboval, C.; Martinez, B.; Ramade, J.; Qu, J.; Triboulin, A.; Cruguel, H.; Baptiste, B.; Klotz, S.; et al. Effect of Pressure on Interband and Intraband Transition of Mercury Chalcogenide Quantum Dots. *J. Phys. Chem. C* **2019**, *123*, 13122–13130.
- (3) Savitzky, A.; J. E. Golay, M. Smoothing and Differentiation of Data by Simplified Least Squares Procedures. *Anal. Chem.* **1964**, *36*, 1639–1643.
- (4) Moghaddam, N.; Gréboval, C.; Qu, J.; Chu, A.; Rastogi, P.; Livache, C.; Khalili, A.; Xu, X. Z.; Baptiste, B.; Klotz, S.; et al. The Strong Confinement Regime in HgTe Two-Dimensional Nanoplatelets. *J. Phys. Chem. C* **2020**, *124*, 23460–23468.